Induction of Hepatocellular Carcinoma Cell Cycle Arrest and Apoptosis by *Dendropanax morbifera* Leveille Leaf Extract via the PI3K/AKT/mTOR Pathway

Gi Dae Kim

Department of Food and Nutrition, Kyungnam University, Changwon, Korea

Liver cancer is prevalent worldwide and associated with a high mortality rate. Therefore, developing novel drugs derived from natural products to reduce the side effects of chemotherapy is urgently needed. In this study, the inhibitory effect of *Dendropanax morbifera* Leveille extract (DME) on growth of hepatocellular carcinoma (HCC) cells and its underlying mechanisms were investigated. DME suppressed the growth, migration, and invasion of SK-Hep1 human HCC cells. It also reduced the expression of the G0/G1 phase regulator proteins cyclin-dependent kinase (CDK) 4, cyclin D, CDK2, and cyclin E, thereby inducing G0/G1 arrest. Moreover, DME treatment reduced the expression of antiapoptotic proteins, including caspase-9, caspase-3, PARP, and Bcl-2 and increased the expression of the proapoptotic protein, Bax. DME also increased reactive oxygen species production and reduced the cellular uptake of rhodamine 123. DME treatment increased the levels of p-p38 and p-FOXO3a in a dose-dependent manner and decreased those of p-PI3K, p-AKT, p-mTOR, and p-p70 in SK-Hep1 cells. In addition, combined treatment with DME and LY294002, an AKT inhibitor, significantly reduced p-AKT levels. In summary, these results show that the PI3K/AKT/mTOR signaling pathway is involved in DME-mediated inhibition of proliferation, migration, and invasiveness, and induction of apoptosis of HCC cells.

Key Words *Dendropanax morbifera* Leveille, Hepatocellular carcinoma, Cell cycle arrest, Apoptosis

INTRODUCTION

Cancer has become a public health burden and is a major cause of morbidity and mortality in middle-aged and older adults worldwide. Hepatocellular carcinoma (HCC) is the sixth most common cancer and the second leading cause of cancer-related deaths worldwide [1,2].

Compounds isolated from natural sources such as plants, marine organisms, and microorganisms have been used to treat various human diseases [3]. According to World Health Organization reports, approximately 80% of people continue to believe in and use natural products as medicines, and certain developed pharmaceuticals are derived from medicinal plants. There is ongoing research on novel compounds from natural resources that have therapeutic potential, resulting in many significant discoveries, including those with antioxidant, anti-inflammatory, analgesic, anti-infective, and anticancer properties [4-6].

One reason for the increased interest in natural compounds is that while most chemically synthesized drugs demonstrate high toxicity against both cancer and normal cells, natural compounds have relatively few side effects or no cytotoxic effects [7]. In particular, discovering novel anticancer agents from traditional medicines has been in focus [8-10]. Although traditional medicine has been used for thousands of years as an important alternative for cancer treatment in Asian countries, including South Korea, the molecular mechanisms underlying the effects of the natural compounds obtained from these medicinal plant extracts remain unclear.

Dendropanax morbifera Leveille, which belongs to the Araliaceae family, is a subtropical evergreen tree of great value worldwide. The main components of *D. morbifera* Leveille are β-selinene and capnellane-8-one, which belong to the sesquiterpene group, members of which have two fused rings. *D. morbifera* Leveille also contains many other compounds that have not yet been identified [11]. The roots, leaves, seeds, and stems of these plants have been widely used in traditional medicine in Korea to treat headaches, infectious diseases,

Check for updates

skin diseases, and other diseases. To date, studies on *D. morbifera* Leveille have reported various biological effects including antidiabetic, antioxidant, and anticancer effects [12-15]. Crude extracts derived from the leaves of *D. morbifera* Leveille demonstrated cytotoxic effects in various cancer cell lines but not in normal cells [16].

Based on these findings, *D. morbifera* Leveille extracts (DME) are currently used in health supplements and as food additives; however, studies establishing their anticancer effects are still insufficient. Rutin and quercetin were reported as the two major flavonoid components of DME [17]. In this study, SK-Hep1 human HCC cells were treated with DME to observe their effects on cancer cell growth, migration, invasion, and apoptosis, and to elucidate the underlying mechanisms.

MATERIALS AND METHODS

Materials
DME was provided by Dr. Chul-yung Choi of Jeonnam Institute of Natural Resources Research. The compound was dissolved in 100% dimethyl sulfoxide (DMSO). A 100 mg/mL stock solution of DME was prepared and stored at −20°C until use. DMSO, MTT, rhodamine 123, verapamil, and horseradish peroxidase (HRP)-conjugated anti-rabbit and anti-mouse antibodies were purchased from Sigma-Aldrich. The apoptosis detection kit was purchased from BD Biosciences. 2′7′-dichlorofluorescein diacetate (H_2DCFDA) was purchased from Molecular Probes. Phospho-specific anti-p38, anti-FOXO3a, anti-PI3K, anti-AKT, anti-mTOR, and p70 antibodies; anti-PI3K, anti-AKT, anti-mTOR, p70, caspase-9, caspase-3, and PARP-specific antibodies; and the AKT inhibitor LY294002 were purchased from Cell Signaling Technology. HRP-conjugated β-actin, p53, p21, cyclin-dependent kinase (CDK) 4, cyclin D, CDK2, cyclin E, Bax, and Bcl-2 antibodies were purchased from Santa Cruz Biotechnology.

Cell culture
The human HCC cell line (SK-Hep1) was purchased from the American Type Culture Collection. Cells were incubated in Dulbecco's modified Eagle's medium (DMEM) supplemented with 10% FBS and 1% antibiotic-antimycotics at 37°C in a 5% CO_2 incubator.

Cell viability assay
SK-Hep1 cell survival upon DME treatment was measured using MTT assay. Cells were plated in 96-well plates and incubated overnight. After removing the media, DMEM with 0 to 100 μg/mL DME was added, and the cells were incubated for 24 to 72 hours. After each timepoint, 20 μL of 5 mg/mL MTT was added to each well and incubated for 4 hours. The medium was removed thereafter, and the reaction was stopped by adding 200 μL of DMSO to each well. Cell viability was measured using a Synergy HTX plate reader (BioTek Instru-

ments, Inc.) and Gen5 by measuring absorbance at 570 nm.

Wound-healing assay to assess migration
Approximately $5 × 10^5$ cells were seeded in six-well plates and incubated for 24 hours. Cells in each well were manually damaged using a P20 pipette tip. Dead cells from the damaged area were washed with fresh media, and new media supplemented with 0 to 40 μg/mL DME and 1% FBS were added to the cells for 24 hours incubation. The images were captured using an inverted microscope equipped with a camera. The wound-healing area was measured using the ImageJ software (National Institutes of Health).

Invasion assay
Cell invasion assays were performed using six-well dishes with Transwell inserts made with 8-μm polycarbonate membranes (Costar; Corning Inc.). Briefly, 1.5 mL of serum-free DMEM with different DME concentrations was added to cells in the upper chamber (BD BioCoat™ Matrigel™ Invasion Chamber; Corning Inc.), whereas cells in the lower chamber were supplemented with DMEM containing 10% FBS. The cells were then incubated at 37°C under 5% CO_2 for 24 hours. For invasion analysis, noninvading cells in the upper chamber were removed using Q-Tips. Cells in the upper chamber that invaded the lower chamber were fixed with 4% paraformaldehyde for 30 minutes and stained with 0.5% crystal violet solution for 30 minutes. Invasive cells were observed under a microscope and quantified using ImageJ software.

Flow cytometry analysis of the cell cycle distribution
The cells were plated in a 100-mm dish and incubated for 24 hours. After confirming cell proliferation to more than 70% density, fresh media supplemented with 0, 10, 20, or 40 μg/mL DME were added to the cells and incubated for 24 hours. Cells were harvested using trypsin/EDTA and fixed overnight with 70% cold ethanol at −20°C. For cell cycle analysis, the fixed cells were centrifuged at 5,000 rpm for 5 minutes at 4°C and washed with cold PBS. Thereafter, 50 μg/mL RNase A was added for 30 minutes at 37°C. The cells were then stained with 50 μg/mL propidium iodide (PI) for 30 minutes at 37°C, and the DNA quantity of the stained cells was analyzed using a FACS Vantage SE flow cytometer and CellQuest software (BD Biosciences).

Apoptosis assay
HCC cell apoptosis in response to DME treatment was assessed according to the protocol provided with the annexin V-fluorescein isothiocyanate (V-FITC) apoptosis detection kit. Briefly, cells were incubated with 0, 10, 20, or 40 μg/mL DME for 24 hours and diluted to $1 × 10^5$ cell/mL using a binding buffer. The cells were then incubated with Annexin V-FITC and PI for 30 minutes in the dark. The DNA content of the stained cells was analyzed using CellQuest Software and a

FACS Vantage SE flow cytometer.

Measurement of intracellular reactive oxygen species accumulation

Intracellular reactive oxygen species (ROS) production was measured using the fluorescent dye H_2DCFDA. SK-Hep1 cells were treated with 0, 10, 20, or 40 μg/mL DME for 24 hours, washed twice with PBS, stained with 20 μM H_2DCF-DA for 30 minutes, and then washed again twice with PBS. H_2DCFDA reacts with ROS to produce the fluorescent product, dichlorofluorescein (DCF). Intracellular DCF levels were quantified using a flow cytometer (BD Biosciences).

Measurement of the mitochondrial membrane potential

Mitochondrial membrane potential was evaluated using rhodamine 123. After treating cells with DME for 24 hours, they were washed with PBS and incubated with 1 μL/mL rhodamine 123 for 60 minutes in the dark. The cells were then washed with PBS, stained with 1 μg/mL PI, and analyzed with a flow cytometer (BD Biosciences). Verapamil (20 μM) was used as a positive control.

Determination of protein expression levels by western blotting

Cells were treated with DME (0, 10, 20, or 40 μg/mL) for 24 hours. Proteins were extracted through a reaction with PRO-PREP Protein Extraction Solution containing protease inhibitors and phosphatase inhibitors (Roche Diagnostics GmbH) for 30 minutes at 4°C, followed by centrifugation at 13,000 rpm at 4°C for 30 minutes. Protein samples (40 μg) were sep-arated by 6% to 12% sodium dodecyl sulfate-polyacrylamide gel electrophoresis and transferred to polyvinylidene fluoride membranes (Bio-Rad Laboratories, Inc.). The membranes were blocked with 5% bovine serum albumin (BSA; AMRES-CO, Inc.) and TBS with 0.1% Tween 20 (TBS-T) for 1 hour and then incubated with primary antibodies (diluted 1:500-1:1,000 with 5% BSA) overnight at 4°C. The membranes were then washed four times with TBS-T for 3 minutes each and incubated with horseradish peroxidase-conjugated anti-rabbit or anti-mouse secondary antibodies (1:1,000) for 1 hour at room temperature. Proteins were visualized using an Advanced Electrochemiluminescence Western Blot Detection Kit (Amersham).

Statistical analysis

The data are presented as the mean ± SD for the indicated number of independently performed experiments. Statistical significance ($P < 0.05$) was determined using Student's t-test for paired data. Statistical analyses were performed using SPSS for Windows version 23 (IBM Corp.).

RESULTS

DME suppressed SK-Hep1 cell proliferation

To confirm the inhibitory effects of DME on human HCC cell growth, SK-Hep1 cells were treated with 0 to 100 μg/mL DME for 24 to 72 hours. The half-maximal inhibitory concentrations (IC_{50}) of DME against SK-Hep1 cells after 24, 48, and 72 hours were 48.9, 18.6, and 11.0 μg/mL, respectively (Fig. 1A). Treatment with 25 μg/mL DME for 24, 48, and 72 hours demonstrated significant suppression of cell prolif-
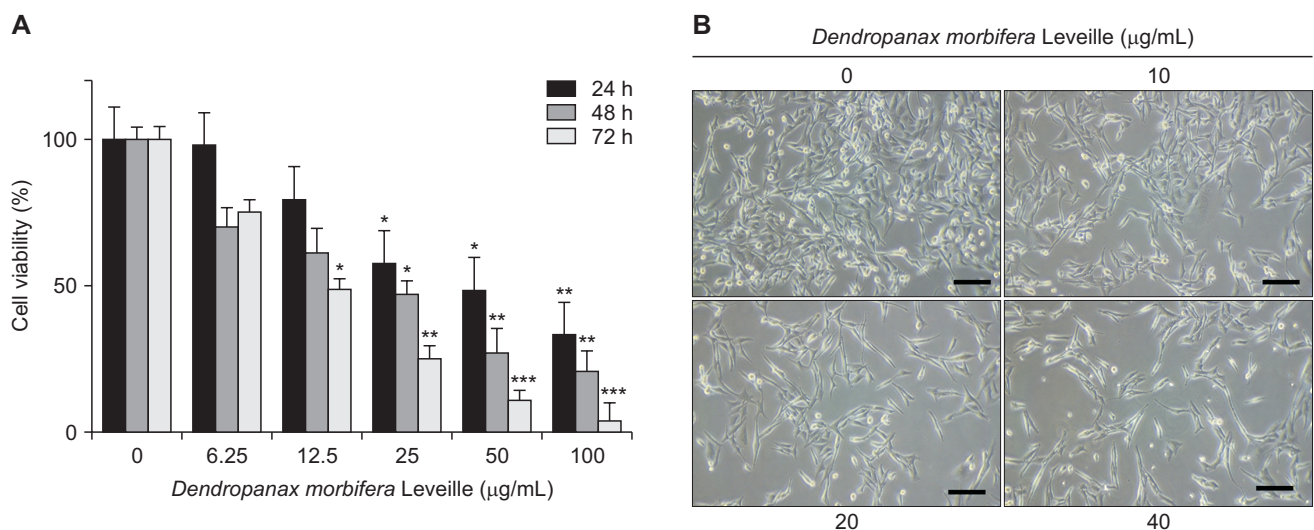

Figure 1. Effects of *Dendropanax morbifera* Leveille extract (DME) on SK-Hep1 cell growth. (A) Cell survival curve after DME treatment. Cells were cultured for 24, 48, and 72 hours with 0, 6.25, 12.5, 25, 50, and 100 μg/mL DME. The cell survival rate was determined by the MTT assay. (B) Morphological changes of DME-treated SK-Hep1 cells. DME suppressed SK-Hep1 cell growth, resulting in decreased cell density. The results are presented as the mean ± SD. Statistical differences were determined using Student's t-tests (*$P < 0.05$, **$P < 0.01$, ***$P < 0.001$ vs. control). Cell morphology was visualized by inverted microscopy (×200). Scale bar = 50 μm.

eration ($P < 0.05$). Moreover, DME treatment for 72 hours significantly suppressed cell proliferation, starting at a concentration of 12.5 μg/mL ($P < 0.05$). In a subsequent study, we confirmed the concentration at which the biological effects were apparent; however, the cytotoxicity was low, based on the IC_{50} concentration and changes in morphology after a 24-hour incubation. DME concentrations up to 40 μg/mL were used for subsequent analyses (Fig. 1B).

DME suppressed SK-Hep1 cell migration and invasion

For migration analysis, a scratch was made in the cells grown in a culture dish at a density of 70%. The cells were then incubated for 24 hours in fresh media with 1% FBS and DME was added at 0, 10, 20, and 40 μg/mL to observe its effect on migration. In Figures 2A and 2B, the wound healing areas were significantly reduced after treatment with 20 μg/mL and 40 μg/mL DME compared to the wound healing area in the control group, with migration rates of 73.5% and 19.2%, respectively ($P < 0.05$). To measure HCC invasion, cells were treated with 0, 10, 20, and 40 μg/mL DME in an 8-μm poly-

carbonate membrane chamber for 24 hours, and the number of cells that invaded the lower chamber was compared to the number in the control group. In Figure 2C, the number of invading cells after treatment with 10, 20, and 40 μg/mL DME was significantly reduced to 55.5, 23.1, and 14.8%, respectively, compared to the control group ($P < 0.05$).

DME induced G0/G1 arrest and apoptosis of SK-Hep1 cells

Since we confirmed the inhibition of SK-Hep1 cell proliferation, migration, and invasion by DME, we performed an additional study to determine the effects of DME on SK-Hep1 cell cycle regulation. As shown in Figure 3, after treatment with 0 to 40 μg/mL DME for 24 hours, a dose-dependent increase in the number of cells in G0/G1 phase was observed. Additionally, the expression of proteins related to the G0/G1 phase was confirmed by western blot analysis. As shown in Figure 3C, DME increased the phosphorylation of p38 and FOXO3a as well as the expression levels of p53 and p21, which are cell cycle regulatory factors. This treatment led to a dose-dependent reduction in the expression of G0/G1 phase regula-
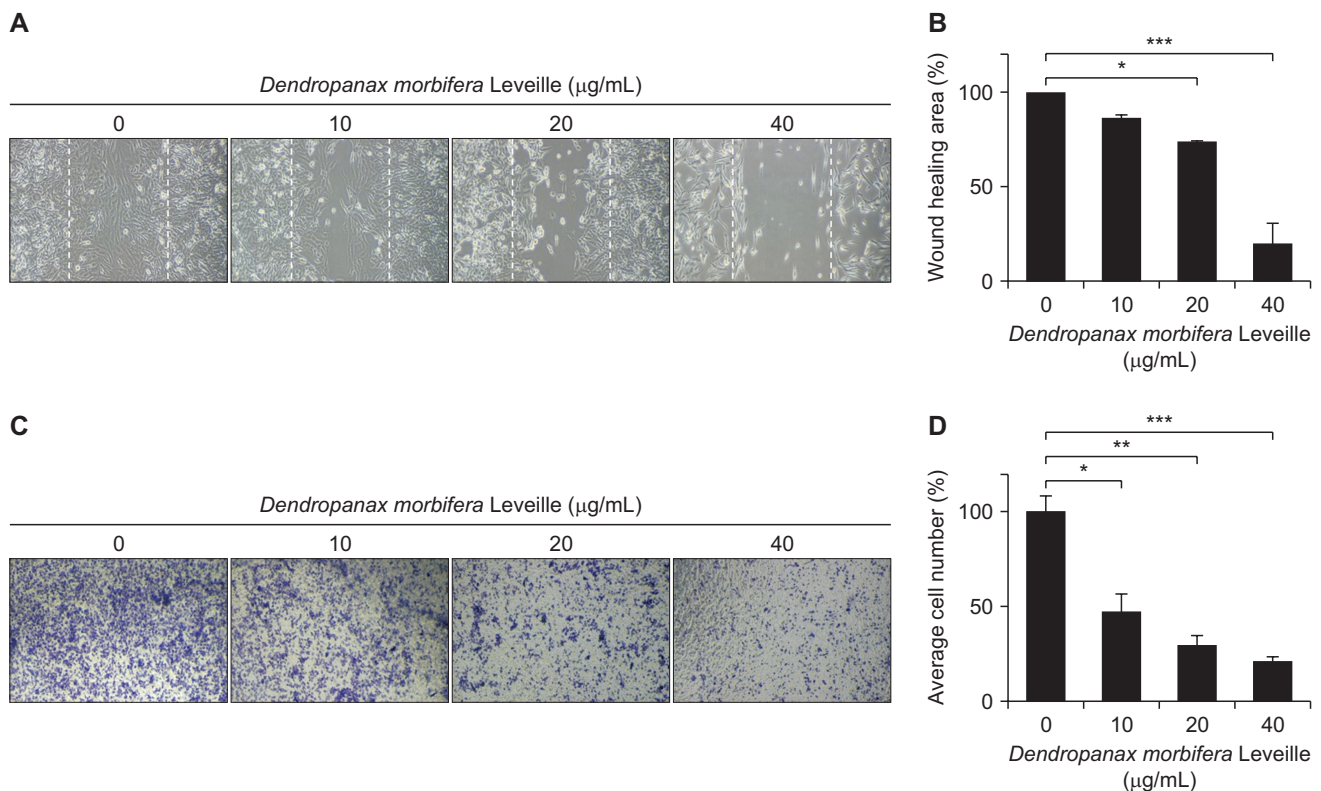

Figure 2. Effects of _Dendropanax morbifera_ Leveille extract (DME) on cell migration and invasion. (A, B) Once cells were confluent on six-well plates, they were wounded with a scratch and treated with various concentrations of DME from 0 to 40 μg/mL. The migration area was measured after 24 hours. Magnification, ×100. (C, D) Cells were added to the upper chamber with 1.5 mL of serum-free Dulbecco's modified Eagle's medium (DMEM), and DMEM with 10% FBS was added to the lower chamber. After incubation for 24 hours, non-invading cells in the upper chamber were removed using a Q-tip, and the cells invading the lower chamber were fixed with 4% paraformaldehyde and stained with 0.5% crystal violet. Invasive cells were then examined under a microscope and quantified using ImageJ (National Institutes of Health). Magnification, ×100. The results are presented as the mean ± SD. Statistical differences were determined using Student's _t_-tests (*$P < 0.05$, **$P < 0.01$, ***$P < 0.001$ vs. control).
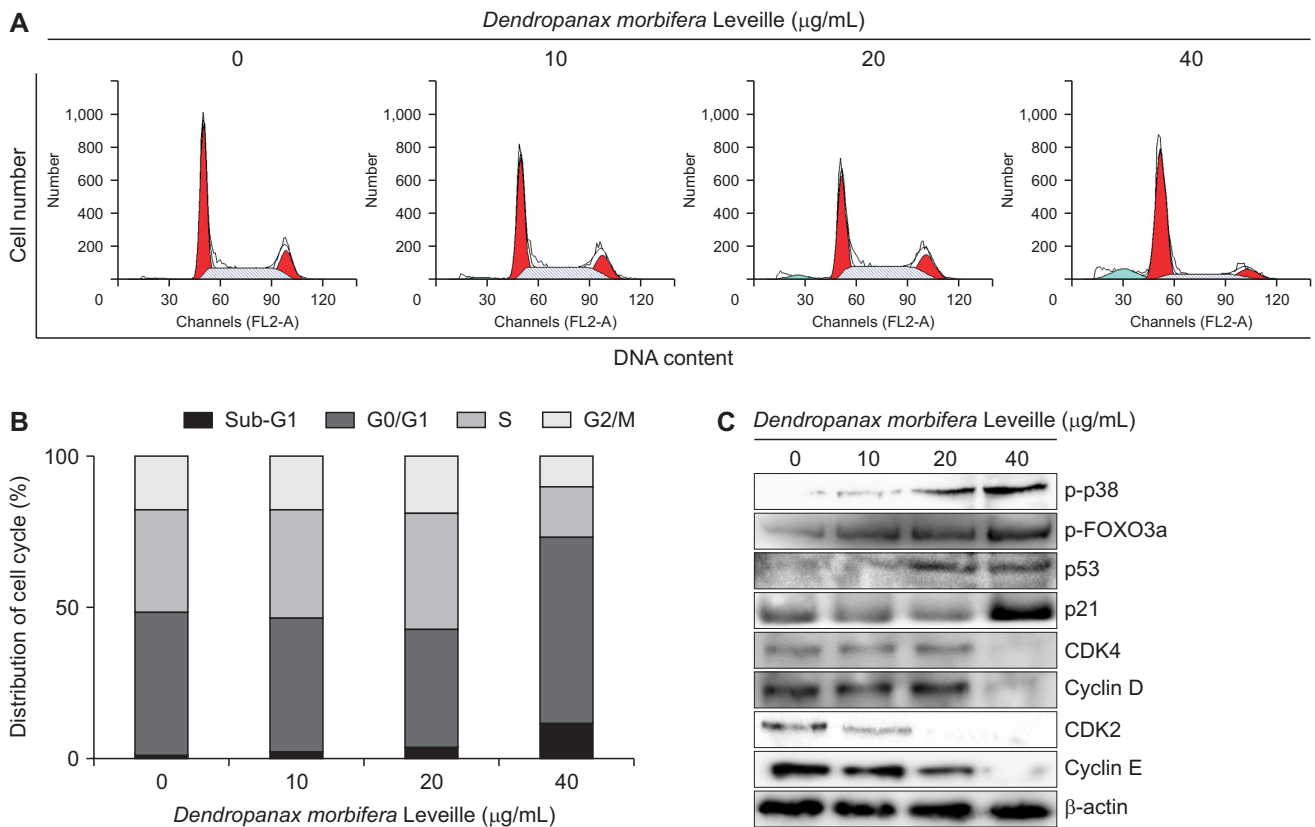
Figure 3. Effects of *Dendropanax morbifera* Leveille extract (DME) on cell cycle progression. (A) After treating cells with 0, 10, 20, or 40 μg/mL DME for 24 hours, they were stained with propidium iodide, and cell cycle progression was confirmed by flow cytometric analyses. (B) Cell cycle distribution in the G0/G1, S, G2/M phases after DME treatment. (C) The expression levels of G0/G1-related proteins, such as p38, FOXO3a, p53, p21, CDK4, cyclin D, CDK2, and cyclin E, were determined using western blotting. β-actin was used as an internal control.

tory proteins, including CDK4, cyclin D, CDK2, and cyclin E, thereby inducing G0/G1 arrest.

Since cell cycle analysis showed a dose-dependent increase in the number of sub-G1 cells at DME concentrations of 10 μg/mL and higher, annexin V-FITC/PI double staining assays were performed to evaluate whether DME treatment could induce apoptosis. Cells treated with 40 μg/mL DME showed a significantly increased the apoptotic cell population by 35.27% ($P < 0.001$; Fig. 4B). To investigate the mechanism underlying the induction of apoptosis, the levels of proapoptotic proteins such as caspase-9, caspase-3, PARP, and Bax, and the antiapoptotic protein Bcl-2, were evaluated using western blotting (Fig. 4C). The levels of antiapoptotic proteins, such as caspase-9, caspase-3, PARP, and Bcl-2, decreased in a dose-dependent manner after DME treatment. The expression of the proapoptotic protein Bax increased in a dose-dependent manner with the induction of apoptosis. Moreover, ROS production increased from 1.38% in the control group to 50.23% in the group treated with 40 μg/mL DME (Fig. 4D).

We then also analyzed whether the induction of ROS production by DME treatment was associated with the regulation of the intracellular mitochondrial membrane potential.

In Figure 4E, the positive control group (20 μM verapamil) had a cellular accumulation of rhodamine 123 by 94.59% compared to the control group (Immunoglobulin G, negative control). However, after treatment with 40 μg/mL DME, this was reduced to 67.17%. A significant reduction in the intracellular accumulation of rhodamine 123 indicates mitochondrial dysfunction due to oxidative stress, which suggests that DME affects mitochondrial membrane potential.

DME regulated the PI3K/AKT/mTOR signaling pathway in SK-Hep1 cells

The PI3K/AKT/mTOR signaling pathway regulates cell survival, proliferation, and migration. We verified that DME regulated the PI3K/AKT/mTOR signaling pathway in SK-Hep1 cells (Fig. 5A and 5B). To evaluate the inhibitory effects on the expression of components of this pathway after DME treatment, western blotting analysis was performed after treatment of SK-Hep1 cells with 0, 10, 20, and 40 μg/mL DME for 24 hours. DME treatment reduced the p-PI3K, p-AKT, p-mTOR, and p-p70 levels. Moreover, LY294002, which is an AKT inhibitor, was combined with either 0 or 40 μg/mL DME to determine whether DME can act as a PI3K/AKT inhibitor (Fig. 5C). DME significantly inhibited p-AKT expression in SK-

A

Dendropanax morbifera Leveille (µg/mL)

Annexin V (FITC)

B

C

Dendropanax morbifera Leveille (µg/mL)

D

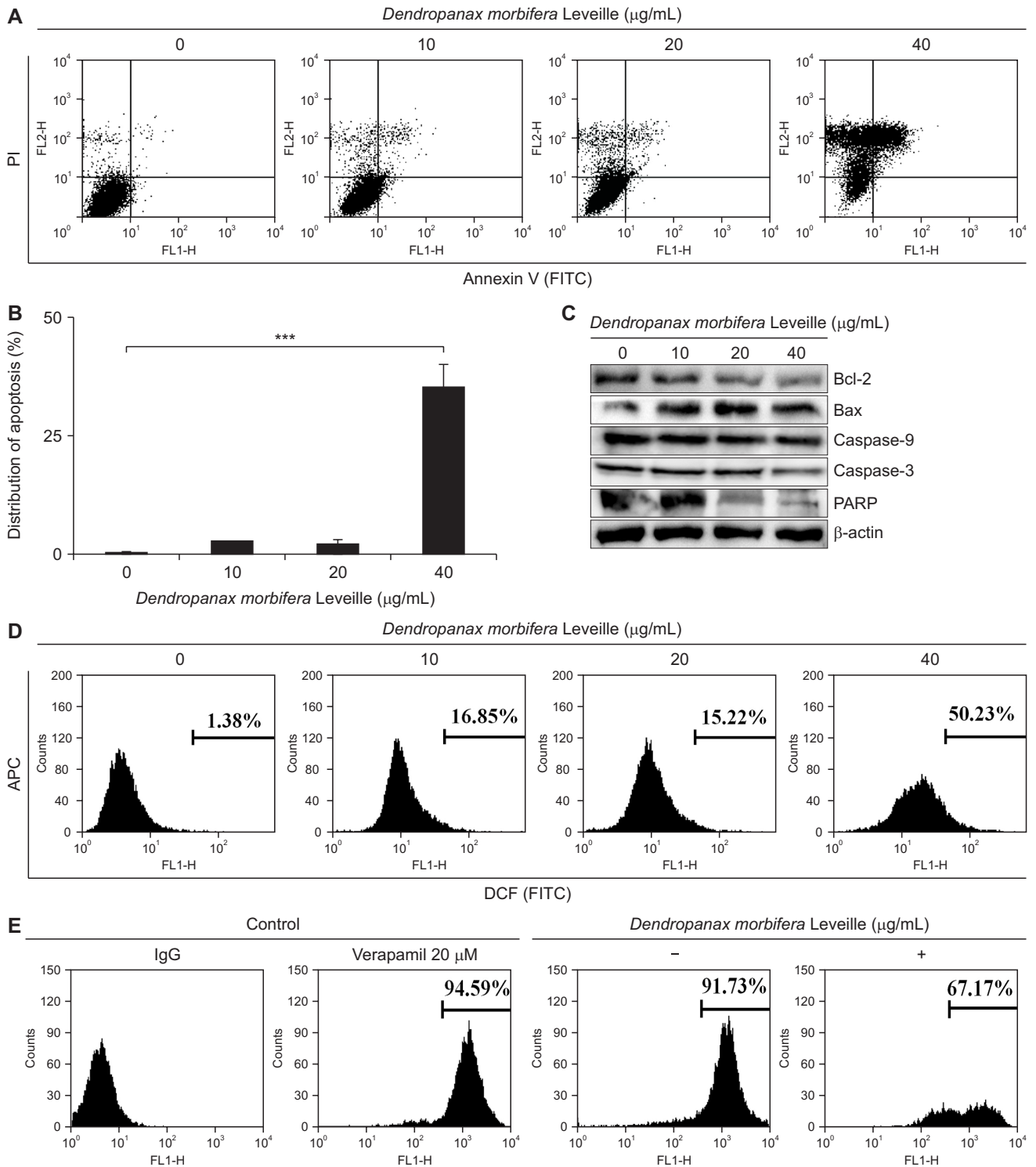Dendropanax morbifera Leveille (µg/mL)

DCF (FITC)

E

Figure 4. Effects of *Dendropanax morbifera* Leveille extract (DME) on ROS production and mitochondrial membrane potential after apoptosis induction. (A, B) Cells were treated with 0, 10, 20, or 40 µg/mL DME for 24 hours, stained with annexin V and propidium iodide (PI), and analyzed using a FACS Calibur flow cytometer (BD Biosciences). (C) The expression levels of proapoptotic and antiapoptotic proteins in apoptosis-induced cells after DME treatment were analyzed using western blotting. (D) Reactive oxygen species generation was measured in cells exposed to 0, 10, 20, and 40 µg/mL DME by adding H_2DCFDA and measuring the fluorescent product, dichlorofluorescein (DCF). (E) Cells were treated with DME or verapamil (positive control) for 24 hours and cultured with rhodamine 123. They were analyzed using a flow cytometer. Data are presented as the mean ± SD of triplicate tests. β-actin was used as an internal control. FITC, fluorescein isothiocyanate; APC, allophycocyamine. ***$P < 0.001$ vs. control.
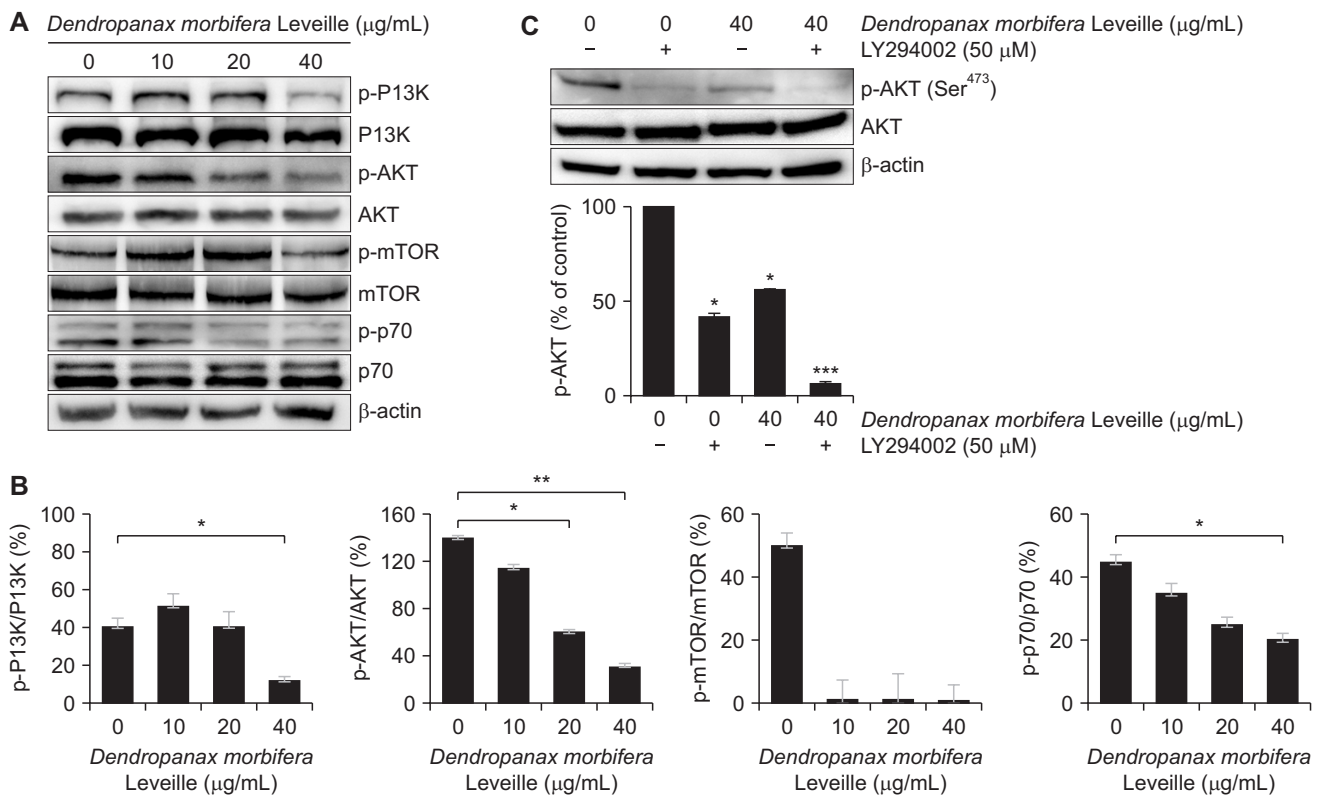
Figure 5. *Dendropanax morbifera* Leveille extract (DME) regulated the PI3K/AKT/mTOR signaling pathway. (A) The expression levels of proteins related to the PI3K/AKT/mTOR signaling pathway were determined using western blotting after treating SK-Hep1 cells with 0, 10, 20, or 40 μg/mL DME for 24 hours. (B) Band intensity was normalized using a total form protein. (C) Cells were treated with 0 or 40 μg/mL DME and the AKT inhibitor LY294002, and the levels of p-AKT were assessed by western blotting analysis. Band intensities were normalized to total AKT. β-actin was used as an internal control. Values indicate the mean ± SD. *$P < 0.05$, **$P < 0.01$ as shown by the Student's *t*-test.

Hep1 cells ($P < 0.05$).

DISCUSSION

Currently available anti-cancer treatments exert anticancer effects via are based on various strategies. Development of novel anticancer drugs derived from natural compounds with low toxicity remains an area of interest. In this study, treatment of SK-Hep1 cells with DME inhibited cancer cell growth by inducing G0/G1 arrest and apoptosis.

p38 is a mitogen-activated protein kinase that links important extracellular signals by regulating cell proliferation, differentiation, migration, and apoptosis [18,19]. Similar to p21, p27, p53, cyclin D, and cyclin B, FOXO3a promotes the expression of its target genes, resulting in cell cycle arrest and growth inhibition in cancer cells [20,21]. The cell cycle is a typical cell division process in eukaryotes. It progresses to four major checkpoints: G1/S, S, G2/M, and spindle assembly [22,23]. Cyclins and CDK complexes play significant roles in regulating cell cycle progression. CDKs and cyclins regulate different cell cycle stages The G1 and S phases are regulated by CDK2, CDK6, CDK4, cyclin D1, and cyclin E, whereas the G2/M phase is regulated by CDK2, cdc2, cyclin

A and cyclin B [24]. This study confirmed that DME induced G0/G1 cell cycle arrest, significantly upregulated p53 and p21 protein levels, and downregulated CDK4, cyclin D, CDK2, and cyclin E levels.

Apoptosis is a spontaneous programmed cell death that occurs under normal physiological and pathological conditions. It is induced in various ways, including death receptors, mitochondrial pathways, and in response to endoplasmic reticulum stress [25,26]. Various factors downregulate prosurvival protein expression while elevating proapoptotic protein levels in the mitochondrial apoptosis pathway, which leads to a decrease in mitochondrial membrane potential and the release of cytochrome *c* from the mitochondria. Cytochrome *c* in the cytoplasm triggers caspase-9 and caspase-3 activation and PARP degradation, eventually leading to apoptosis [27]. The Bcl-2 family of proteins play an important role in apoptosis [28]. This involves a reduction in the levels of antiapoptotic proteins, such as Bcl-2 and Bcl-xL, in the mitochondrial membrane and an increase in the levels of proapoptotic proteins, such as Bax.

The flow cytometry results showed that the rate of apoptosis in SK-Hep1 cells increased in a dose-dependent manner in response to DME treatment. Moreover, western blotting

results showed that the expression levels of caspase-9, caspase-3, PARP, and Bcl-2 decreased and the expression level of Bax increased, demonstrating apoptosis as a result of DME treatment. ROS play important roles in apoptosis. In cancer cells, high levels of endogenous oxidative stress lead to increased ROS production, which inhibits cancer growth [29]. Under pathological conditions, excessive ROS damage DNA, proteins, mitochondria, and the endoplasmic reticulum and can induce cell cycle arrest and apoptosis [30,31]. In this study, we confirmed that ROS production increased in a dose-dependent manner after DME treatment.

The PI3K/AKT/mTOR signaling pathway is an important cellular signaling pathway. It plays a pivotal role in cell proliferation, growth and survival, and angiogenesis by affecting the activities of downstream molecules and is closely related to the development and progression of cancer in humans. AKT signaling induces cell proliferation and blocks apoptosis, by regulating expression/activity of apoptotic proteins, including those belonging to the Bcl-2 family [32]. FOXO3a is an important target of the PI3K/AKT signaling pathway [33,34] and regulates cell cycle arrest by activating transcriptional targets such as p27 and p21 [35]. In this study, deactivation of the PI3K/AKT/mTOR pathway regulated p38 and FOXO3a, thereby downregulating CDK4, cyclin D, CDK2, and cyclin E, and resulting in G0/G1 cell cycle arrest. It also increases the expression of p53, resulting in the regulation of Bcl-2, Bax, caspase-9, caspase-3, and PARP expression, leading to apoptosis.

Natural compounds with anticancer activities exert their effects by targeting various signaling pathways. Many studies have demonstrated the functional roles of various bioactive compounds in the prevention of HCC via the regulation of the PI3K signaling pathway. PI3K inhibition is a key area of HCC prevention [36-38]. DME acts as an inhibitor of the PI3K/AKT/mTOR signaling pathway and decreases the levels of p-AKT after treatment in combination with an AKT inhibitor.

In conclusion, we confirmed that DME inhibited cell proliferation by inducing cell cycle arrest and apoptosis in HCC (SK-Hep1) cells. DME treatment altered cell cycle distribution by increasing the proportion of cells in the G0/G1 phase. Moreover, it regulates the expression of Bcl-2 family proteins and proteins related to the mitochondria, resulting in apoptosis. Moreover, treatment with a combination of DME and an AKT inhibitor decreased the levels of p-AKT, and it was confirmed that inhibition of the PI3K/AKT/mTOR signaling pathway in SK-Hep1 cells was involved in contributed to DME-induced cell cycle arrest and apoptosis. Based on these findings, we suggest that DME has the potential to treat liver cancer.

ACKNOWLEDGMENTS

We thank Dr. Chul-yung Choi for technical support and for providing the materials used in the experiments.

CONFLICTS OF INTEREST

No potential conflicts of interest were disclosed.

ORCID

Gi Dae Kim, https://orcid.org/0000-0002-8149-5361

REFERENCES

1. Calderaro J, Ziol M, Paradis V, Zucman-Rossi J. Molecular and histological correlations in liver cancer. J Hepatol 2019;71:616-30.
2. Heimbach JK, Kulik LM, Finn RS, Sirlin CB, Abecassis MM, Roberts LR, et al. AASLD guidelines for the treatment of hepatocellular carcinoma. Hepatology 2018;67:358-80.
3. Talib WH, Daoud S, Mahmod AI, Hamed RA, Awajan D, Abuarab SF, et al. Plants as a source of anticancer agents: from bench to bedside. Molecules 2022;27:4818.
4. Tang F, Yan HL, Wang LX, Xu JF, Peng C, Ao H, et al. Review of natural resources with vasodilation: traditional medicinal plants, natural products, and their mechanism and clinical efficacy. Front Pharmacol 2021;12:627458.
5. Kumar A. Phytochemistry, pharmacological activities and uses of traditional medicinal plant Kaempferia galanga L. - an overview. J Ethnopharmacol 2020;253:112667.
6. Sultana S, Asif HM. Review: medicinal plants combating against hypertension: a green antihypertensive approach. Pak J Pharm Sci 2017;30:2311-9.
7. Mukherjee AK, Basu S, Sarkar N, Ghosh AC. Advances in cancer therapy with plant based natural products. Curr Med Chem 2001;8:1467-86.
8. Liu Y, Yang S, Wang K, Lu J, Bao X, Wang R, et al. Cellular senescence and cancer: focusing on traditional Chinese medicine and natural products. Cell Prolif 2020;53:e12894.
9. Loizzo MR, Tundis R, Menichini F, Statti GA, Menichini F. Hypotensive natural products: current status. Mini Rev Med Chem 2008;8:828-55.
10. Nwodo JN, Ibezim A, Simoben CV, Ntie-Kang F. Exploring cancer therapeutics with natural products from African medicinal plants, part II: alkaloids, terpenoids and flavonoids. Anticancer Agents Med Chem 2016;16:108-27.
11. Kim HR, Chung HJ. Chemical characteristics of the leaves and the seeds of Korean Dendropanax (Dendropanax morbifera Lev.). J Korean Soc Agric Chem Biotechnol 2000;43:63-6.
12. Moon HI. Antidiabetic effects of dendropanoxide from leaves of Dendropanax morbifera Leveille in normal and streptozotocin-induced diabetic rats. Hum Exp Toxicol 2011;30:870-5.

13. Choi JH, Kim S. Antioxidant and antithrombotic properties of Dendropanax morbifera Léveille (Araliaceae) and its ferments produced by fermentation processing. J Food Biochem 2019;43:e13056.

14. Lee JW, Park C, Han MH, Hong SH, Lee TK, Lee SH, et al. Induction of human leukemia U937 cell apoptosis by an ethanol extract of Dendropanax morbifera Lev. through the caspase-dependent pathway. Oncol Rep 2013;30:1231-8.

15. Balakrishnan R, Cho DY, Su-Kim I, Choi DK. Dendropanax morbiferus and other species from the genus Dendropanax: therapeutic potential of its traditional uses, phytochemistry, and pharmacology. Antioxidants (Basel) 2020;9:962.

16. Setzer WN, Green TJ, Whitaker KW, Moriarity DM, Yancey CA, Lawton RO, et al. A cytotoxic diacetylene from Dendropanax arboreus. Planta Med 1995;61:470-1.

17. Jung MA, Oh KN, Choi EJ, Oh DR, Kim YJ, Bae D, et al. In vitro and in vivo androgen regulation of Dendropanax morbiferus leaf extract on late-onset hypogonadism. Cell Mol Biol (Noisy-le-grand) 2018;64:20-7.

18. Wagner EF, Nebreda AR. Signal integration by JNK and p38 MAPK pathways in cancer development. Nat Rev Cancer 2009;9:537-49.

19. Zheng GZ, Zhang QH, Chang B, Xie P, Liao H, Du SX, et al. Dioscin induces osteosarcoma cell apoptosis by upregulating ROS-mediated P38 MAPK signaling. Drug Dev Res 2023;84:25-35.

20. Nasimian A, Farzaneh P, Tamanoi F, Bathaie SZ. Cytosolic and mitochondrial ROS production resulted in apoptosis induction in breast cancer cells treated with Crocin: the role of FOXO3a, PTEN and AKT signaling. Biochem Pharmacol 2020;177:11399.

21. Liu H, Deng H, Jian Z, Cui H, Guo H, Fang J, et al. Copper exposure induces hepatic G0/G1 cell-cycle arrest through suppressing the Ras/PI3K/Akt signaling pathway in mice. Ecotoxicol Environ Saf 2021;222:112518.

22. Sánchez I, Dynlacht BD. New insights into cyclins, CDKs, and cell cycle control. Semin Cell Dev Biol 2005;16:311-21.

23. Hochegger H, Takeda S, Hunt T. Cyclin-dependent kinases and cell-cycle transitions: does one fit all? Nat Rev Mol Cell Biol 2008;9:910-6.

24. Smith HL, Southgate H, Tweddle DA, Curtin NJ. DNA damage checkpoint kinases in cancer. Expert Rev Mol Med 2020;22:e2.

25. Goldar S, Khaniani MS, Derakhshan SM, Baradaran B. Molecular mechanisms of apoptosis and roles in cancer development and treatment. Asian Pac J Cancer Prev 2015;16:2129-44.

26. Carneiro BA, El-Deiry WS. Targeting apoptosis in cancer therapy. Nat Rev Clin Oncol 2020;17:395-417.

27. Gogvadze V, Orrenius S, Zhivotovsky B. Mitochondria as targets for cancer chemotherapy. Semin Cancer Biol 2009;19:57-66.

28. Zhou F, Yang Y, Xing D. Bcl-2 and Bcl-xL play important roles in the crosstalk between autophagy and apoptosis. FEBS J 2011;278:403-13.

29. Chen X, Dai X, Zou P, Chen W, Rajamanickam V, Feng C, et al. Curcuminoid EF24 enhances the anti-tumour activity of Akt inhibitor MK-2206 through ROS-mediated endoplasmic reticulum stress and mitochondrial dysfunction in gastric cancer. Br J Pharmacol 2017;174:1131-46.

30. Simon HU, Haj-Yehia A, Levi-Schaffer F. Role of reactive oxygen species (ROS) in apoptosis induction. Apoptosis 2000;5:415-8.

31. Kim WS, Lee KS, Kim JH, Kim CK, Lee G, Choe J, et al. The caspase-8/Bid/cytochrome c axis links signals from death receptors to mitochondrial reactive oxygen species production. Free Radic Biol Med 2017;112:567-77.

32. Zhang J, Yu XH, Yan YG, Wang C, Wang WJ. PI3K/Akt signaling in osteosarcoma. Clin Chim Acta 2015;444:182-92.

33. Sunters A, Fernández de Mattos S, Stahl M, Brosens JJ, Zoumpoulidou G, Saunders CA, et al. FoxO3a transcriptional regulation of Bim controls apoptosis in paclitaxel-treated breast cancer cell lines. J Biol Chem 2003;278:49795-805.

34. Link W. Introduction to FOXO biology. Methods Mol Biol 2019;1890:1-9.

35. Taniguchi K, Ii H, Kageyama S, Takagi H, Chano T, Kawauchi A, et al. Depletion of gamma-glutamylcyclotransferase inhibits cancer cell growth by activating the AMPK-FOXO3a-p21 axis. Biochem Biophys Res Commun 2019;517:238-43.

36. Narayanankutty A, Nair A, Illam SP, Upaganlawar A, Raghavamenon AC. Curcumin enriched VCO protects against 7,12-dimethyl benz[a] anthracene-induced skin papilloma in mice. Nutr Cancer 2021;73:809-16.

37. Sheela DL, Narayanankutty A, Nazeem PA, Raghavamenon AC, Muthangaparambil SR. Lauric acid induce cell death in colon cancer cells mediated by the epidermal growth factor receptor downregulation: an in silico and in vitro study. Hum Exp Toxicol 2019;38:753-61.

38. Sachdeva V, Roy A, Bharadvaja N. Current prospects of nutraceuticals: a review. Curr Pharm Biotechnol 2020;21:884-96.